PHYSICAL REVIEW B VOLUME 44, NUMBER 22 1 DECEMBER 1991-II

Rapid Communications

Rapid Communications are intended for the accelerated publication of important new results and are therefore given priority treatment both in the editorial office and in production. A Rapid Communication in **Physical Review B** *should be no longer than 4 printed pages and must be accompanied by an abstract. Page proofs are sent to authors.*

Electron-paramagnetic-resonance and fluorescence-line-narrowing measurements of the lasing center in Cr-doped forsterite

K. R. Hoffman, J. Casas-Gonzalez,* S. M. Jacobsen, and W. M. Yen
Department of Physics and Astronomy, The University of Georgia, Athens, Georgia 30602
(Received 2 August 1991)

We present results of EPR and near-infrared fluorescence-line-narrowing experiments performed on Cr-doped forsterite. The optical measurements permit identification of the signals in the complex EPR spectrum due to the near-infrared lasing center. The site symmetry of the lasing center is shown to be c_s with the mirror plane being in the crystallographic *ab* plane. The magnetic *z* axes of the two magnetically inequivalent sites are in the mirror plane at an angle of $\pm 43°$ to the *b* axis. In addition, the relative energies of the ground-state triplet have also been measured and can be written in terms of spin Hamiltonian energy parameters: $D = +2.20$ and $E = -0.149$ cm^{-1}.

Since the demonstration of near-infrared (NIR) laser action in the title compound, considerable effort has been employed to elucidate the nature of the luminescent center.[1-3] Forsterite contains three different sites that can be occupied by cation impurities. One octahedral site has inversion symmetry (c_i) and two sites, one octahedral and one tetrahedral, have mirror plane symmetry (c_s).[4] Previous EPR studies have identified non-Kramers Cr cations occupying octahedral sites.[5] However, the NIR center is thought to be located in the tetrahedral site.[6] Due to the complex nature of the host, complementary experimental techniques are required to obtain a clear understanding of the NIR center. EPR spectroscopy is an important tool for probing the ground-state structure and site symmetry of paramagnetic defects in crystals. However, the technique has the drawback that when several sites of the same symmetry are present, it is sometimes difficult to assign observed signals to a specific site. Fluorescence line narrowing (FLN) is an optical technique which permits the resolution of closely spaced energy levels normally obscured by inhomogeneous broadening. In addition, FLN measurements made in the presence of a magnetic field permit the field dependence of these levels to be measured.

By combining these two techniques, the EPR signal due to the NIR active center in Cr-doped forsterite can be unambiguously assigned. From our results we conclude that the optical center is located at a site with mirror-plane point symmetry. In addition, the ground-state structure is compatible with the model of Cr^{4+} ions in distorted tetrahedral sites where the $^3A_2$ is the lowest level. However, the hyperfine structure corresponding to the coupling of the magnetic electron with the 9% abundant ^{53}Cr isotope was not observed in the EPR signal corresponding to the NIR center, presumably because the splitting is smaller than the linewidth.

Two crystals were used in this investigation. Crystal *A* was provided by B. Denker (Soviet Academy of Sciences) and crystal *B* was grown by Mitsui of Japan. Both crystals were grown in oxidizing atmosphere and showed the absorption bands associated with the lasing center. The concentration of the NIR active center is higher in crystal *B*.

The EPR experiments were performed using a Bruker ESR200D Spectrometer with a TE_{102} cavity operating at *x* band (9.45 GHz) with a 100-kHz magnetic-field modulation. For measurements made at low temperatures, between 4 and 30 K, we employed an Oxford Instruments model ESR 900 cryostat. For the temperature-dependent measurements, power levels as low as 10 nW were used to avoid saturation.

The FLN measurements employed a Raman shifter to achieve coherent radiation with a 0.5-cm^{-1} linewidth in the region of 1.09–1.1 μm. R6G dye laser output was shifted by 8310 cm^{-1} using the second-order Stokes shift of H_2 gas at 550 psi. The dye laser and first-order Stokes shift were removed from the beam by a Schott RG-1000 filter. The magnetic field was supplied by a Varian electromagnet capable of 3.0 T between the pole faces. All optical measurements were made with a polished and oriented crystal cut from boule *A*. The emission was dispersed by a 1.8-m Jarrell Ash 78-400 monochrometer capable of 0.01 cm^{-1} resolution. The light was detected with a Varian VPM-157A photomultiplier. The electronic signal was measured with a Stanford Research Boxcar integrator and stored in a microcomputer. To achieve the high resolution necessary for these measurements the slits of the spectrometer were opened to 40 μm. For all measurements the pump beam polarization was parallel to the *b* axis.

We have found in both crystals *A* and *B*, three distinct EPR signals consistent with non-Kramers ions. Two of the signals clearly show the hyperfine structure corresponding to the ^{53}Cr isotope and have been discussed previously in terms of being either Cr^{2+} or Cr^{4+} in octahedral sites.[5] Signal intensity permitting a thorough study of the third EPR signal due to a non-Kramers ion was obtained only in sample *B*. Apparently, the intensity of this EPR signal grows with increasing concentration of the NIR center. This third signal is broader than the other two with a linewidth of the order 30 G. No hyperfine structure was observed for this center. Assuming the ground state is a spin triplet, the observed transitions are between the spin states $S_z = \pm 1$. These transitions are allowed due to transverse components in the oscillating magnetic field.

The rotational diagram of the third EPR signal, shown in Fig. 1, corresponds to rotating the magnetic field in the *ab* and *bc* planes. We note that the signal intensities are much lower for rotations in the *ab* plane than in the *bc* plane. The rotational diagram in the *bc* plane shows the magnetic *z* axis of the site is in the *ab* plane. The observation of two resonances in the rotational diagram in *ab* plane is a result of there being two magnetically inequivalent sites. The figure shows the magnetic axes are pointing approximately $\pm 45°$ from the *b* axes. The removal of the degeneracy with rotations in the *bc* plane is due to slight misalignment of the field with the plane.

The zero field FLN spectra obtained by resonantly pumping into levels 1 and 2 of the excited state triplet are labeled i and ii, respectively, in Fig. 2.[7] The pump laser

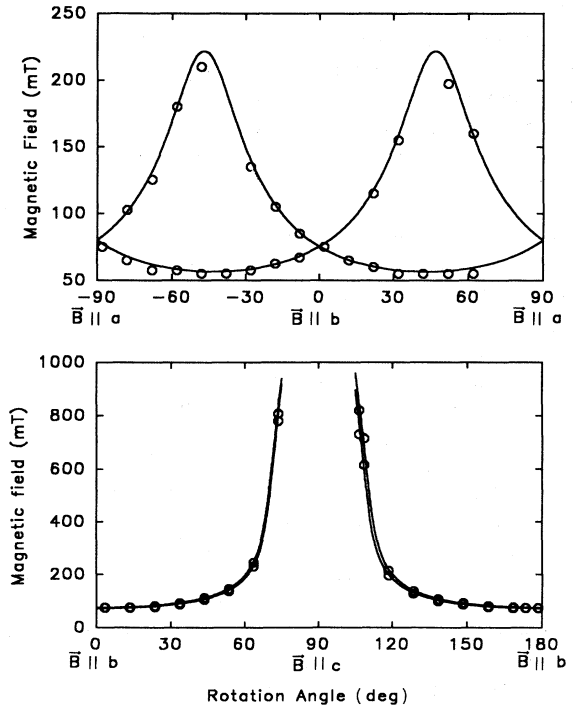

FIG. 1. The rotational diagrams in the *ab* and *bc* planes for Cr:forsterite. The open circles are the data and the solid curves are the fits generated by Eq. (1).

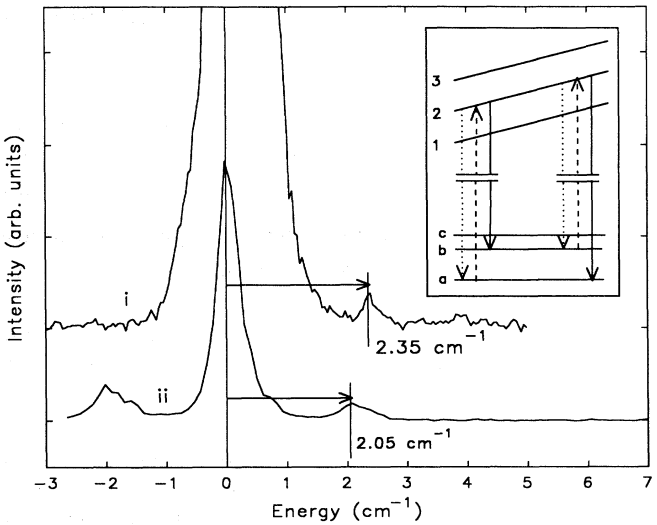

FIG. 2. The resonant FLN data obtained by pumping into the lowest NIR excited state (i) and the middle NIR excited state (ii). The inset shows the transitions involved in producing the spectrum for process ii. The slope of the excited states reflects the inhomogeneous broadening in the crystal.

energy is set equal to 0. Also labeled in the graph are the energy splittings between the ground-state levels: 2.05 and 2.35 ± 0.02 cm^{-1}. The transitions responsible for the signal measured in ii are shown in the inset. For process i, the nonresonant peak is three orders of magnitude weaker than the resonant signal and reflects the weak absorption from level 1 to the excited state. A nonresonant peak at higher energy, similar to that in process ii is not observed due to thermal depopulation of level 3 at 1.5 K. In process ii the resonant and nonresonant peaks have intensities of the same order because transitions to both levels 1 and 2 are strong. Also, the measurements were made at a slightly higher temperature, thereby permitting the peak at higher energy to be observed. The linewidth of the nonresonant signal indicates that the resolution is limited by the pump laser.

The magnetic field dependence of the FLN signal measured with the laser in resonance with level 1 of the excited state (process i) is shown in Fig. 3. The application of a magnetic field increases the separation of the resonant and nonresonant lines. In addition, at higher fields a complex set of peaks separate from the resonant signal due to field-induced transitions involving ground-state level *b*. From these measurements, the field dependence of the energy splitting between the levels *a* and *c* of the ground-state triplet can be determined. Similar measurements made in resonance with level 2 of the excited state allow the determination of the field dependence of the energy splitting between levels *a* and *b* of the ground state. The structure that appears in the spectra corresponding to transitions involving level *b* of the ground state is due to the center occupying magnetically inequivalent sites in the lattice. The field dependence of the ground-state level splittings are plotted in Fig. 4 along with theoretical fits. The theoretical curves show the energies for three different orientations of the applied field relative to the

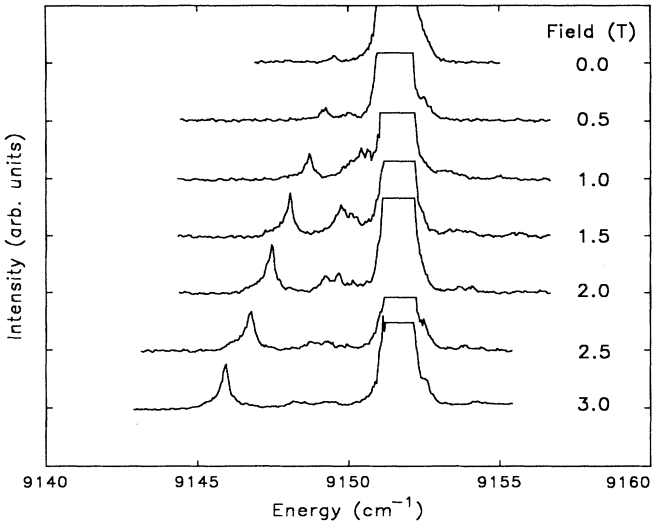

FIG. 3. The resonant FLN signal for process i when a magnetic field is applied along the b axis. The sample temperature is ~ 1.7 K.

site magnetic axis: 38°, 43°, and 48°.

We have successfully fit the experimental evolution of the EPR lines with the magnetic field orientation to the following spin Hamiltonian:

$$\mathcal{H} = g\mu_B \mathbf{B}\cdot\mathbf{S} + D[S_z^2 - \tfrac{1}{3}S(S+1)] + E(S_x^2 - S_y^2). \quad (1)$$

The following relations between the magnetic x, y, and z axes and the crystalline a, b, and c axes were chosen: x coincides with c and z is rotated $\pm 43°$ from b in the ab plane. The other parameters used to generate the solid curves in Fig. 1 have the following values: effective spin $S=1$, $g=1.93$, $D=2.2$ cm^{-1}, and $E=-0.149$ cm^{-1}.

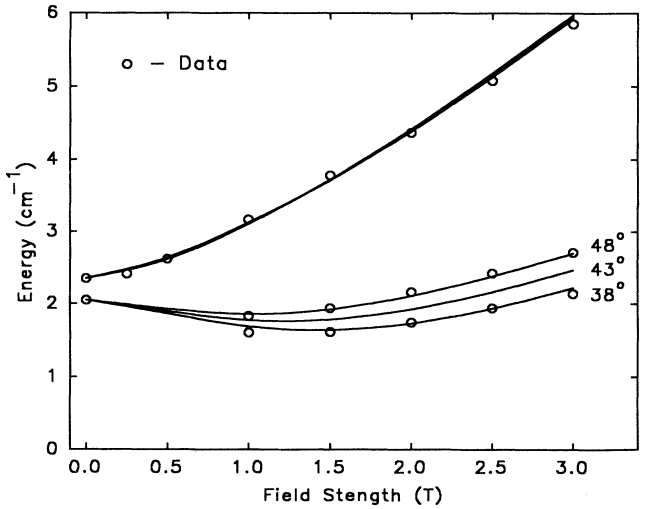

FIG. 4. The relative energies of the three ground-state energies in the applied magnetic field. The solid curves are generated using Eq. (1) for various angles between the magnetic z axis and the applied field. Note the splitting between levels a and c is insensitive to the angle.

The choice of a positive value of D is discussed below. The fitted curves for rotation in the bc plane include the effects of slight misorientation of the applied field and plane.

The temperature dependence of the EPR signal intensity for the NIR center lines has also been measured. The signal intensity is proportional to the population difference between the $|m_s|=1$ levels. The temperature effects will be different depending on whether the doublet is at higher or lower energy than the third level in the ground state. Therefore, these measurements determine the sign of the splitting parameter D and permit its magnitude to be approximated. The results show that D is positive and of magnitude 2.2 ± 0.3 cm^{-1}.

The resonant FLN experiments can be explained in terms of selection rules in absorption and emission.[6] The only transition strongly allowed to level 1 of the excited state is from level c in the ground state. Therefore, the nonresonant emission is very weak. This signal is due to weak resonant absorption from level a followed by the allowed emission to level c. Hence, FLN measurements resonant with the lowest excited state allow the splittings between levels a and c to be measured. Similarly, when the laser is resonant with the excited state level 2, the energy splitting between levels a and b can be measured. In the case of the level 2 the transition strengths to levels a and b are of the same order; therefore, the resonant and nonresonant signal intensities are similar. The energy parameters D and E are determined from FLN measurements to be 2.20 ± 0.02 and 0.15 ± 0.02 cm^{-1}, respectively.

The field dependence of the energy levels has been modeled theoretically using the spin Hamiltonian described previously. The field mixes the levels so that the transitions to all levels in the ground state are somewhat allowed. Therefore the new lines that appear in process i in an applied field are due to absorption from level b and emission to level c. The new peaks are a measure of the energy difference $E(c)-E(b)$ which will be shown to be sensitive to orientation of the magnetic field. The energy-level splittings were calculated for various orientations of the applied field to the magnetic axis of the center. As seen in Fig. 4, the position of the middle level is the only one sensitive to the rotation angle. By plotting the relative energies between levels at several angles, the orientation of the magnetic sites in the applied field can be determined. The graph in Fig. 4 indicates that the applied field was misaligned with the magnetic axis 38° in one site and 48° in the other site. The simulations suggest that a magnetic field applied along the b axis would be at a 43° angle to the magnetic axis of both sites. This is consistent with the EPR results further substantiating the correlation between the measurements. It is this orientation dependence that explains the structural lines that appear in Fig. 3 at higher fields.

The experimental results show that the EPR signal and the optical spectra are associated with the same defect. The ground state of this center consists of three levels corresponding to a system with an effective spin $S=1$. The $|m_s|=1$ levels are split by $2\times(0.149$ cm$^{-1})$ and centered at energy 2.20 cm^{-1} above the $m_s=0$ level. The orientation of the magnetic axes referred to the crystalline axes

as well as the zero field splittings have been proven to be the same for both measurements.

This structure for the ground state is compatible with the proposed model for the center by Petričević, Gayen, and Alfano consisting of a Cr^{4+} ion substituting for Si^{4+} ions at tetrahedral sites. The $^3A_2$ ground-state level would be expected to have small splittings because the spin-orbit interaction is a second-order effect. However, the observation of the hyperfine interaction in the EPR signal is required to clearly identify the defect as a Cr ion.

We thank Professor Denker for providing us with sample *A* and V. Petričević and R. R. Alfano for kindly loaning sample *B* for these measurements. We also thank T. V. Morgan for the use of the EPR spectrometer. We are indebted to R. S. Meltzer for many helpful discussions and use of his laboratory for some of the optical experiments. One of us (J.C.-G.) would like to thank D.G.I.C.Y.T. of Spain for Grant No. BE91-040. Partial support for this work was also provided by DARPA Grant No. N00014-90-J-4088.

---

*Permanent address: Departamento de Fisica de la Materia Condensada, Facultad de Ciencias, Plaza de S. Francisco s/n, 50009 Zaragoza, Spain.

[1]V. Petričević, S. K. Gayen, and R. R. Alfano, Appl. Phys. Lett. **52**, 1040 (1988).

[2]H. R. Verdun, L. M. Thomas, D. M. Andrauskas, and T. McCollum, Appl. Phys. Lett. **53**, 2593 (1988).

[3]R. Moncorgé, G. Cormier, D. J. Simkin, and J. A. Capobianco, IEEE J. Quantum Electron. **27**, 114 (1991).

[4]Weiyi Jia, Huimin Liu, S Jaffe, W. M. Yen, and B. Denker, Phys. Rev. B **43**, 5234 (1991).

[5]J. Casas-Gonzalez, S. M. Jacobsen, K. R. Hoffman, and W. M. Yen, in *OSA Proceedings on Advanced Solid State Lasers,* edited by G. Dubé and L. Chase (Optical Society of America, Washington, DC, 1991), Vol. 10, p. 64.

[6]V. Petričević, S. K. Gayen, and R. R. Alfano, Appl. Phys. Lett. **53**, 2590 (1988).

[7]K. R. Hoffman, S. M. Jacobsen, J. Casas-Gonzalez, and W. M. Yen, in *OSA Proceedings on Advanced Solid State Lasers* (Ref. 5), p. 44.